Journal of Biomechanics 48 (2015) 651–658

Contents lists available at ScienceDirect

Journal of Biomechanics

journal homepage: www.elsevier.com/locate/jbiomech
www.JBiomech.com

Mechanical characterization of stomach tissue under uniaxial tensile action

Z.G. Jia, W. Li*, Z.R. Zhou

Tribology Research Institute, Key Laboratory for Advanced Technology of Materials of Ministry of Education, Southwest Jiaotong University, Chengdu 610031, China

ARTICLE INFO

Article history:
Accepted 26 December 2014

Keywords:
Porcine stomach
Tensile test
Stress relaxation
Strain creep
Fracture
Anisotropy

ABSTRACT

In this article, the tensile properties of gastric wall were investigated by using biomechanical test and theoretical analysis. The samples of porcine stomach strips from smaller and greater curvature of the stomach were cut in longitudinal and circumferential direction, respectively. The loading-unloading, stress relaxation, strain creep, tensile fracture tests were performed at mucosa-submucosa, serosa-muscle and intact layer, respectively. Results showed that the biomechanical properties of the porcine stomach depended on the layers, orientations and locations of the gastric wall and presented typical viscoelastic, nonlinear and anisotropic mechanical properties. During loading-unloading test, the stress of serosa-muscle layer in the longitudinal direction was 15–20% more than that in the circumferential direction at 12% stretch ratio, while it could reach about 40% for the intact layer and 50% for the mucosa-submucosa layer. The results of stress relaxation and strain creep showed that the variation degree was obviously faster in the circumferential direction than that in the longitudinal direction, and the ultimate residual values were also different for the different layers, orientations and locations. In the process of fracture test, the serosa-muscle layer fractured firstly followed by the mucosa-submucosa layer when the intact layer was tested, the longitudinal strips firstly began to fracture and the required stress value was about twice as much as that in the circumferential strips. The anisotropy and heterogeneity of mechanical characterization of the porcine stomach were related to its complicated geometry, structure and functions. The results would help us to understand the biomechanics of soft organ tissue.

1. Introduction

Minimally invasive surgery (MIS) is a focus and development trend of the surgery, due to these merits such as micro-traumatic, less bleeding, short wound healing time, rapid recovery after operation, and short hospitalization et al. (Bos et al., 2013; De et al., 2007; Marucci et al., 2000). However, minimally invasive devices such as forceps could cause soft tissue injury when clamping force is excessive, while small clamping force easily cause grasper and tissue slipping as dragging tissue operation. Hence, the safety operation at the interface of minimally invasive devices and soft tissue is necessary in the MIS. From the perspective of biomechanics, the biomechanics characteristics of soft tissue have very important guiding significance to study the interaction mechanism of minimally invasive devices and soft tissue. However, due to the complex geometry and structure of soft tissue, especially viscera organs, it is difficult to study their biomechanical properties.

The stomach is a multifunctional organ that controls nutrient and drug delivery to the intestines. It grinds, mixes, stores liquid and semisolid chyme, and releases content into the duodenum at a rate controlled by nutrient-stimulated duodeno-gastric reflexes (Horowitz et al., 1994; Pal et al., 2004). Therefore, the mechanical characterization of the stomach is essential to understand physiological functions of gastric accommodation and mechanosensation, or to provide mechanical data for the MIS operation on the stomach. On the investigation of the mechanical behavior of the stomach, some studies in animal and human stomach measured pressure-volume relations for evaluation of tone, compliance and tension in the gastric fundus by using a barostat (Azpiroz and Malagelada, 1985; Whitehead et al., 1997). The main assumptions made in these studies were that the mechanical properties in all directions and different layers were the same and that the wall was infinitely thin. Other studies on the stomach of the pig, rat and rabbit have demonstrated that the mechanical properties of the stomach are location-dependent, direction-dependent and species-dependent due to its geometric and structural complexity (Liao et al., 2005; Zhao et al., 2005, 2008). Egorov et al. (2002) reported that the tensile properties of the human cadaver stomach were the following: the values of maximal stress and destructive strain for stomach axial specimens were 0.7 MPa and 190%, for stomach transversal specimens

* Corresponding author. Tel.: +86 28 8763 4270; fax: +86 28 8760 3142.
E-mail address: liweijiani@home.swjtu.edu.cn (W. Li).

http://dx.doi.org/10.1016/j.jbiomech.2014.12.048
0021-9290/

were 0.5 MPa and 190%. In addition, some studies revealed the mechanical properties of the digestive organs. Lyons et al. reported that the porcine intestines showed a peak extrusion force ranging from 9 N to 14.8 N when pushed through a 13 mm hole in extrusion test, and similar extrusion properties between cleaned and uncleaned fresh porcine intestines were observed. Furthermore, viscoelastic testing (7.5 mm/min, 15 mm/min and 30 mm/min) showed little rate dependency in the extrusion properties for the porcine intestines (Lyons et al., 2013). Although the mechanical properties of the stomach have conducted in some researches, little current data is available about the influence of its anisotropy and heterogeneity on the biomechanical properties.

Therefore, in the present work, the uniaxial tensile properties of gastric wall at the different layers, orientations, and locations were investigated by using biomechanical test and theoretical analysis to study the mechanical anisotropy and heterogeneity of the stomach. The results would help us understand the biomechanics of soft organ tissue and provide experimental data to investigate the interaction mechanism of minimally invasive devices and soft tissue.

2. Materials and methods

2.1. Experimental materials

Excised fresh porcine stomach was chosen as an experimental model for this study due to its structural and functional similarity to the human stomach. The test stomach models were taken from three pigs of a local pig slaughterhouse. The weight of the pigs was about 140 kg and the age was18–20 weeks. The three stomach models were preserved in an icebox and transported to the laboratory within 1 h postmortem, and tested within 4 h after extraction to avoid dehydration. The stomach models were dissected along the middle of the smaller curvature and gently washed by using saline (Fig. 1). The stomach wall test samples were taken from the gastric smaller curvature and greater curvature. Then the stomach wall samples were cut into strips in the longitudinal direction (parallel to the direction of gastric mucosal fold of the greater curvature or the smaller curvature) and the circumferential direction (perpendicular to the direction of gastric mucosal fold of the greater curvature or the smaller curvature), respectively, as shown in Fig. 1. The strips were divided to two groups in the same sampling position of greater or smaller curvature. In order to study the mechanical properties of different layers of gastric wall, one group was separated into mucosa-submucosa layer and serosa-muscle layer, and another group was non-separated (Intact layer). Each group had three strip samples, and each strip was about 120 mm long and 10 mm wide. All samples were prepared and tested at a nominal room temperature of 20 ± 3 °C and relative humidity of $60 \pm 5\%$. During the tests, the stomach strip samples were sprayed with physiological saline every half an hour to simulate their surface moisture in the body.

2.2. Experimental equipment

The biomechanical tests were carried out using a microcomputer control electronic universal material testing machine (HY0580, Shanghai Hengyi Testing Machine Co., Ltd., China), which was usually used to conduct the mechanical tests of soft tissues such as tensile, compression, laceration, peeling trial et al., as shown in Fig. 2. The HY0580 is composed of a force transducer (Transcell Technology Inc., America), a full digital AC servo motor (Panasonic MINAS A4 SERIES Corp., Japan), a high precision synchronous speed reducer and four differently shaped clamps. The force transducer's resolution is 0.01% and its measurement range is from 1 mN to 100 N. The displacement accuracy is $\leq 0.2\%$ and the displacement range is up to 800 mm. The test speed range is 0.001 to 500 mm/min. It is fully computer-controlled and a sampling rate is at 50 samples per seconds to data files. The testing repeatable accuracy is $\leq 0.5\%$.

2.3. Experimental method

While testing, the stripe sample was fixed on the fixtures of the HY0580 (Fig. 2). Both ends of the stripe sample were wrapped

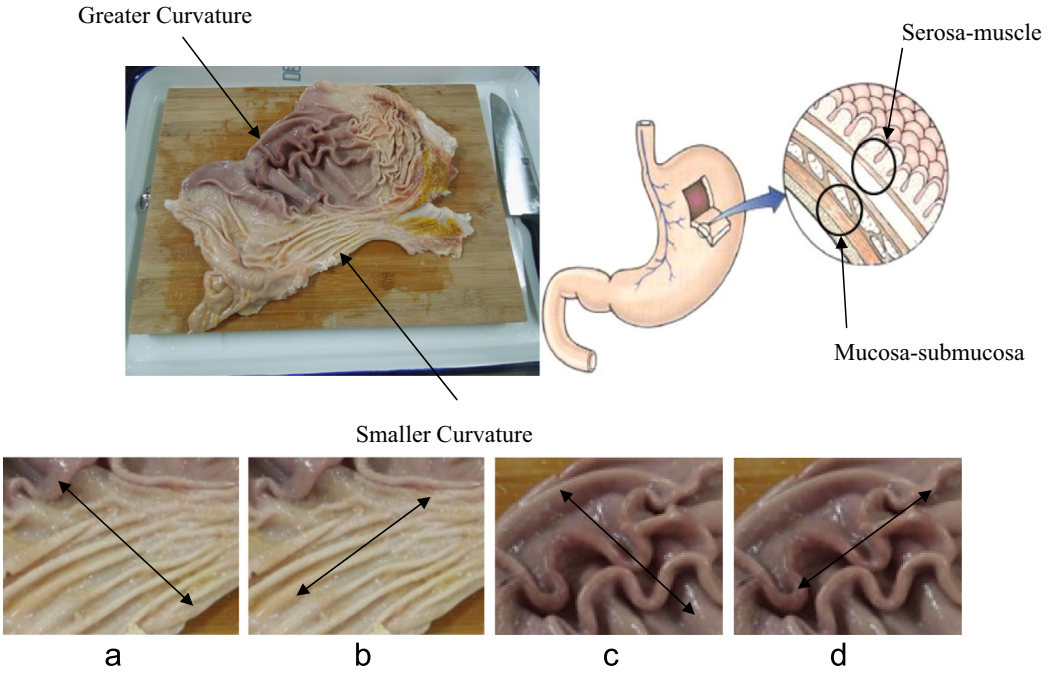

Fig. 1. Porcine stomach and gastric wall structure and the definition of circumferential and longitudinal direction, (a) Circumferential direction of smaller curvature, (b) Longitudinal direction of smaller curvature, (c) Circumferential direction of greater curvature, (d) Longitudinal direction of greater curvature.

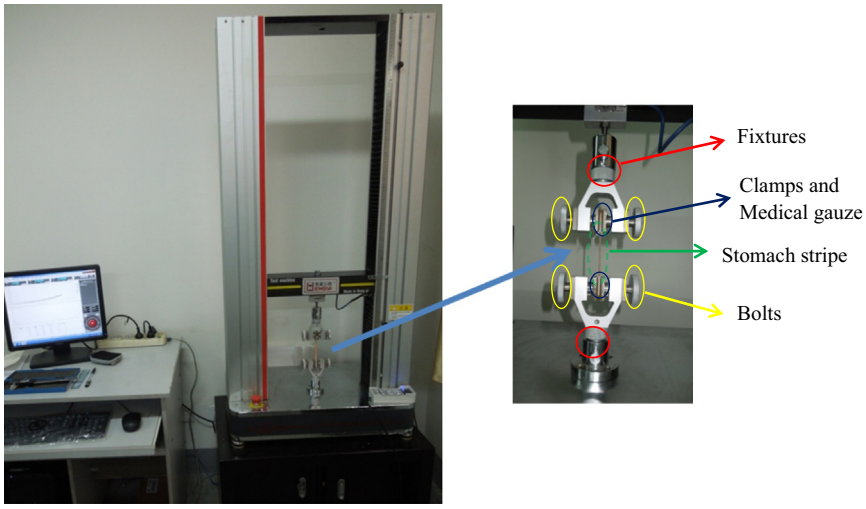

Fig. 2. HY0580 electronic universal material testing machine, setup with fixtures and stomach stripe sample.

Table 1
Parameters of loading-unloading tests.

Location	Different layer	Circumferential direction		Longitudinal direction		V/	S/
		B_0/mm	H_0/mm	B_0/mm	H_0/mm	mm/s	mm
Smaller curvature	Serosa-muscle	9.92 ± 0.02	3.07 ± 0.03	9.84 ± 0.02	2.76 ± 0.01		
	Mucosa-submucosa	9.66 ± 0.01	2.74 ± 0.02	9.54 ± 0.08	2.97 ± 0.03	1	12
	Intact layer	10.13 ± 0.01	5.77 ± 0.03	10.09 ± 0.01	5.63 ± 0.08		
Greater curvature	Serosa-muscle	10.12 ± 0.06	3.94 ± 0.01	9.86 ± 0.02	3.94 ± 0.08		
	Mucosa-submucosa	9.96 ± 0.04	2.74 ± 0.03	9.68 ± 0.06	2.58 ± 0.01	1	12
	Intact layer	10.12 ± 0.02	6.68 ± 0.02	10.04 ± 0.08	6.46 ± 0.03		

with medical gauze and then fixed in the clamps of the fixtures to prevent tissue slippage. The bolts of the clamps were tightened by using a torque wrench to 0.3 N-m to prevent tissue damage when clamping, which were similar to the tighten bolts of grip with a torque wrench of 0.2 N-m to fix the porcine rectus sheath in Lyons et al.'s study (Lyons et al., 2014). The clamps position of the fixtures can be adjusted to ensure that the stripe sample was in the natural extension state. The size of the stripe sample was measured by using a Vernier caliper with the accuracy of $\pm$ 0.02 mm. The original test length (L_0) of each sample was 100 mm. The original thickness (B_0) and width (H_0) were the mean of the triple measured values. The stripe sample size, tensile speed (V), elongation (S) and time (T) of keeping the stretched length under loading-unloading, stress relaxation, strain creep, and tensile failure tests are listed in Table 1–3. The tensile speed (V) was 1 mm/s in the loading-unloading and tensile failure tests, while it was 6 mm/s in the stress relaxation and strain creep tests, which simulated the general and maximum stomach wall dragging speed of MIS, respectively. The elongation (S) was 12 mm, which simulated the stomach wall dragging elongation of MIS. According to the principle of the viscoelastic property of biological tissue, preconditioning should be done before tensile tests (Fung, 1993). The preconditioning behavior was believed to be due to strain softening (a non-viscoelastic behavior observed during preconditioning) in the tissue in response to the loading (Gregersen and Kassab, 2002). Three cycles of loading-unloading tests were done for each stripe sample. The typical stress-stretch ratio curves of stripe sample in loading-unloading test are shown in Fig. 3. The curves of the first two cycles did not overlap, which were for preconditioning the stripe sample mechanically. The differences of the third cycle curve basically disappeared compared with the second curve, which was used for the data analysis. The subsequent tensile tests were conducted immediately after the precondition.

2.4. Mechanical data analysis

According to Lagrange concept, the stress was defined as tension force divided by the initial cross sectional area.

The stress and stretch ratio in a gastric wall strips were computed as

$$\text{Stress}: \quad S = \frac{F_t}{A_0} \tag{1}$$

Where F_t is the recorded tension force, and A_0 is the initial cross-sectional area (computed from the stripe sample thickness H_0 and width B_0 as $A_0 = B_0 H_0$).

$$\text{Stretchratio}: \quad \lambda = \frac{L_t - L_0}{L_0} \times 100\% \tag{2}$$

Where L_t is the recorded elongation length, and L_0 is the original test length ($L_0 = 100$mm).

$$\text{Stressratio}: \delta = \frac{S_t}{S_0} \tag{3}$$

The δ is defined as normalized function. Where S_t is the recorded stress, and S_0 is the original stress.

In the loading-unloading, stress relaxation and strain creep tests, the experimental data were presented by the mean and standard deviation. F test (analysis of variance) was used to determine the significant difference among three porcine stomach samples under the same test conditions. Independent "t" test was used to compare the thickness of the serosa-muscle and mucosa-submucosa layer. The level of statistical significance was set to $P < 0.05$.

Table 2
Parameters of stress relaxation and creep tests.

	Location	Different layer	Circumferential direction		Longitudinal direction		V/	T/
			B_0/mm	H_0/mm	B_0/mm	H_0/mm	mm/s	s
Relaxation tests	Smaller curvature	Serosa-muscle	9.82 ± 0.01	2.94 ± 0.04	10.08 ± 0.06	3.06 ± 0.03		
		Mucosa-submucosa	9.56 ± 0.08	2.84 ± 0.03	9.52 ± 0.01	2.88 ± 0.05	6	300
		Intact layer	10.18 ± 0.03	5.72 ± 0.01	10.25 ± 0.06	5.80 ± 0.09		
	Greater curvature	Serosa-muscle	10.02 ± 0.01	3.78 ± 0.05	10.02 ± 0.01	3.78 ± 0.05		
		Mucosa-submucosa	9.48 ± 0.05	2.68 ± 0.06	9.48 ± 0.05	2.68 ± 0.06	6	300
		Intact layer	10.22 ± 0.01	6.30 ± 0.02	10.22 ± 0.01	6.30 ± 0.02		
Creep tests	Smaller curvature	Serosa-muscle	9.68 ± 0.05	2.42 ± 0.01	9.96 ± 0.03	2.98 ± 0.04		
		Mucosa-submucosa	9.40 ± 0.02	2.86 ± 0.03	9.58 ± 0.05	2.74 ± 0.01	6	300
		Intact layer	9.92 ± 0.06	5.28 ± 0.05	10.28 ± 0.03	5.66 ± 0.02		
	Greater curvature	Serosa-muscle	9.30 ± 0.01	3.32 ± 0.02	9.84 ± 0.02	3.44 ± 0.06		
		Mucosa-submucosa	9.46 ± 0.08	2.52 ± 0.01	9.66 ± 0.02	2.54 ± 0.08	6	300
		Intact layer	9.86 ± 0.06	5.84 ± 0.06	10.04 ± 0.03	5.94 ± 0.01		

Table 3
Parameters of tensile failure tests.

Layer	Different location	Circumferential direction		Longitudinal direction		V/ mm/s
		B_0/mm	H_0/mm	B_0/mm	H_0/mm	
Intact layer	Smaller curvature	9.62 ± 0.02	5.74 ± 0.05	9.94 ± 0.03	5.56 ± 0.06	1
	Greater curvature	9.38 ± 0.06	6.02 ± 0.04	9.80 ± 0.01	6.18 ± 0.08	

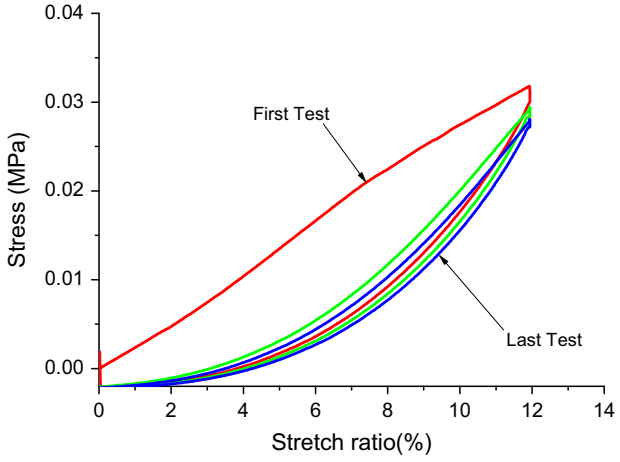

Fig. 3. Typical stress-stretch ratio curves of stripe sample in loading-unloading test.

3. Results

Under the tensile conditions of loading-unloading speed of 1 mm/s and elongation length of 12 mm (Table 1), the mean stress-stretch ratio curves of stomach stripes at different layers, orientations and locations in the loading-unloading tensile tests are shown in Fig. 4. It was obviously that the curves of tensile stress with stretch ratio were significantly different among different layers, orientations and locations. In all loading-unloading tests, the tensile stress under the same stretch ratio was the maximum for serosa-muscle layer and the minimum for mucous-submucosa layer, while the tensile stress of the intact layer was intermediate values between the two layers. The tensile stress in the longitudinal direction was higher than that in the circumferential direction. Similarly, the tensile stress of stomach stripes from the greater curvature was higher than that in the smaller curvature. These results indicated that the stomach strips from the serosa-muscle layer of greater curvature and in the longitudinal direction were stiffer and not more deformable.

3.1. Stress relaxation properties

When the stomach stripes were stretched at a speed of 6 mm/s to achieve the preset elongation length of 12 mm, and then remained the preset elongation and kept 300 s (Table 2), the mean stress ratio-time curves (had been normalized) of stomach stripes at different layers, orientations and locations in the stress relaxation tests are shown in Fig. 5(a) and (b). The significant stress relaxation phenomena occurred when the stretch ratio was held to a constant, which was called partial stress relaxation in this study because the residual stress was above zero when the duration time got to 300 s. The higher stress relaxation rate appeared in the first 100 s, and it was about 70% of the total. In all stomach stripes from the smaller curvature or greater curvature, the degree of stress relaxation in the circumferential direction was larger than that in the longitudinal direction. By contrast, the degree of stress relaxation was the largest in the mucosa-submucosa layer, the smallest in the serosa-muscle layer, and between the two was the intact layer. These results indicated that the stomach stripes in the circumferential direction and the mucosa-submucosa layer were more deformable.

3.2. Creep properties

When the stomach stripes were stretched at a speed of 6 mm/s to achieve the preset stress of 0.05 MPa, and then remained the preset stress and kept 300 s (Table 2.), the mean stretch ratio-time curves (had been normalized) of stomach stripes at different layers, orientations and locations in the creep tests are shown in Fig. 5(c) and (d). The creep curves showed that the stretch ratio increased with time when the samples were applied the constant stress. The higher variation of stretch ratio also appeared in the first 100 s, and it was about 70% of the total. In all stomach stripes from the smaller curvature or greater curvature, the variation of stretch ratio in the circumferential direction was larger than that in the longitudinal direction. By contrast, the variation of stretch ratio was the largest in the mucosa-submucosa layer, the smallest in the serosa-muscle layer, and between the two was the intact

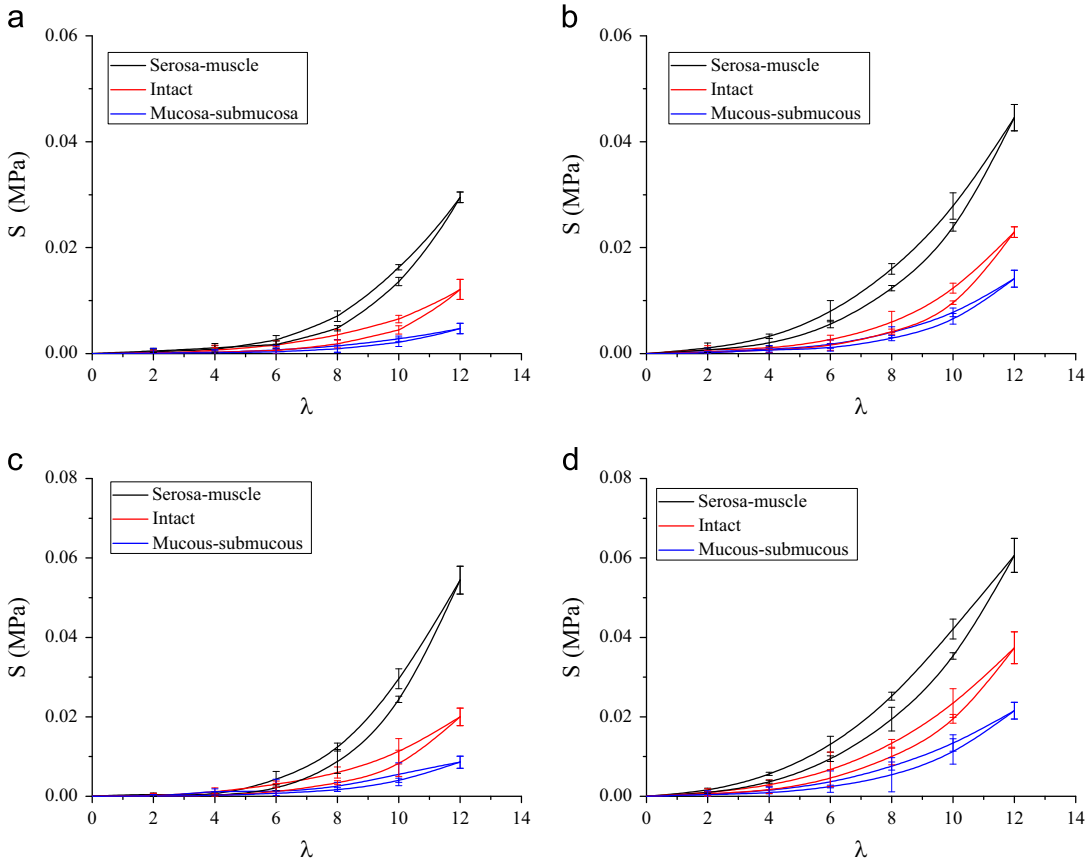

Fig. 4. Stress-stretch ratio curves of stomach stripes at different layers, orientations and locations, (a) Stomach stripes from smaller curvature and in the circumferential direction, (b) Stomach stripes from smaller curvature and in the longitudinal direction, (c) Stomach stripes from greater curvature and in the circumferential direction, (b) Stomach stripes from greater curvature and in the longitudinal direction.

layers. These results corresponded with the results of the stress relaxation tests.

3.3. *Tensile failure properties*

When the stomach stripes were stretched at a speed of 1 mm/s (Table 3), the representative tensile fracture curves of the intact stomach stripes at different orientations and locations in the tensile fracture tests are shown in Fig. 6 (To facilitate the reading of the results, the tensile fracture curves of one stomach stripe can be seen, which correspond to the mean curves). The stress (S) and stretch ratio (λ) of the three stomach stripes at the several critical failure points (A, B, C and D) had no significant differences ($P < 0.05$). According to the values of these critical failure points, the tensile fracture stress value in the longitudinal direction was about twice as much as the circumferential direction, while the fracture stretch ratio in the longitudinal direction was only about a third of that in the circumferential direction. These results illustrated that the stomach stripe could withstand the tensile deformation in the circumferential direction. Furthermore, the fracture test was a continuous process, in which the serosa-muscle layer fractured first, followed by the mucosa-submucosa layer. Thus, the tensile failure stress curves fluctuated with the stretch ratio.

4. Discussion and conclusions

In the present work, the uniaxial tensile properties of gastric wall at the different layers, orientations, and locations were investigated by using loading-unloading, stress relaxation, strain creep, and tensile failure tests. The purpose was to study the effect of the anisotropy and heterogeneity of stomach on the biomechanical properties of the tissue. Test results showed that the biomechanical properties of stomach tissue depended on the layers, orientations and locations of the gastric wall. In loading-unloading tests, the stress response showed a hysteresis loop for each cycle, and a stiffening effect with stretch ratio was always observed. According to the deformation of samples at the same stretch ratio, the serosa-muscle layer was stiffer than the mucous-submucosa layer, the stripes in the longitudinal direction were stiffer than that in the circumferential direction, and the stripes from the greater curvature were stiffer than that from the smaller curvature. The stress relaxation tests and creep tests are two of the most important evaluation ways used for determining viscoelastic properties of materials, and they are also one of the important means to study and verify the relationship between biological phenomena of biological tissues and organs and environment mechanical stimulation. In the stress relaxation and strain creep tests, the largest amount of variation appeared in the initial 100 s, and it could reach a 70% of the initial value. The variation degrees of the mucous-submucosa strips were larger than that of the serosa-muscle strips, the circumferential stripes were larger than the longitudinal stripes, and the smaller curvature strips were larger than the greater curvature strips. In the process of fracture tests, the serosa-muscle layer fractured firstly followed by the mucosa-submucosa layer, the longitudinal strips firstly began to fracture and the required stress value was about twice as much as that in the circumferential strips. The above results showed that the mechanical properties of stomach tissue were anisotropy and heterogeneity. The present study can provide useful information to explore an effective method to identify safe thresholds during grasping and palpation tasks in MIS, which can guide a surgeon to manipulate stomach wall with minimal resulting damage. In addition, the experimental data can help us deeply research the interaction mechanism of minimally invasive devices

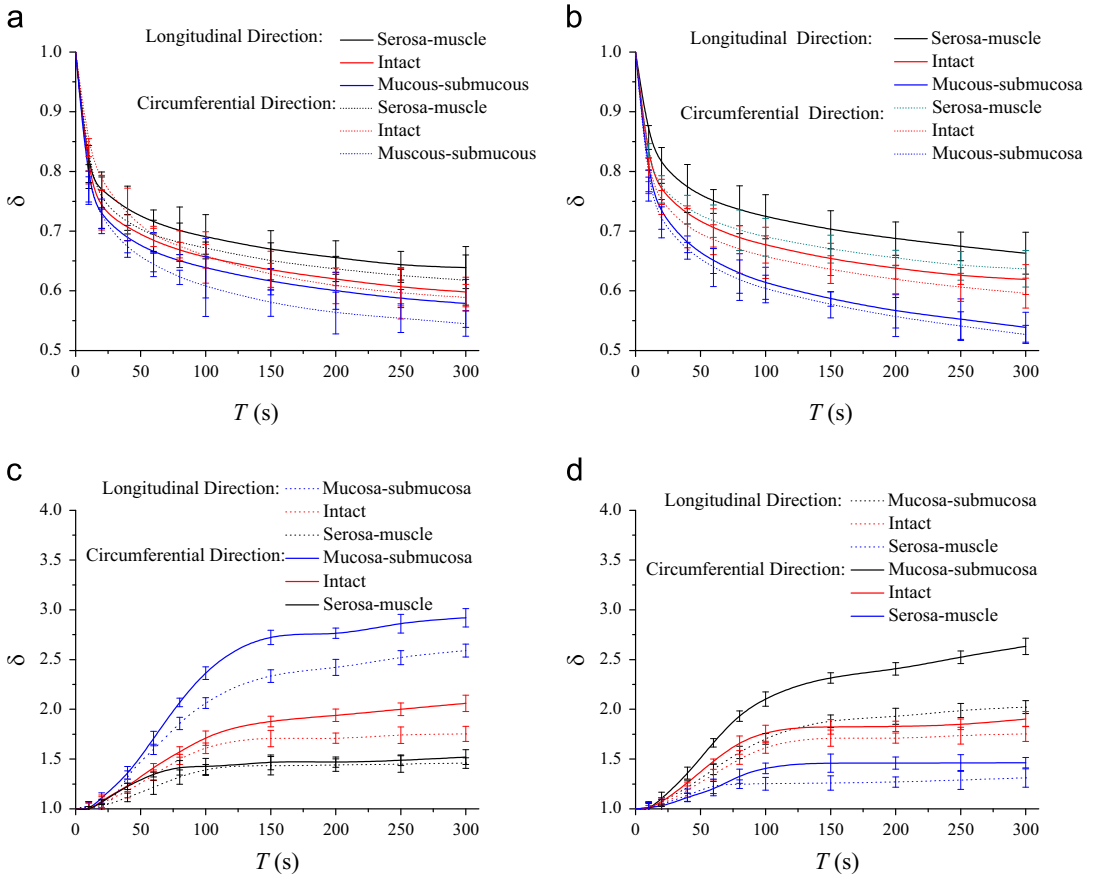

Fig. 5. Stress relaxation and creep curves of stomach stripes at different layers, orientations and locations, (a) Stress relaxation curves from smaller curvature, (b) Stress relaxation curves from greater curvature, (c) Creep curves from smaller curvature, (d) Creep curves from greater curvature.

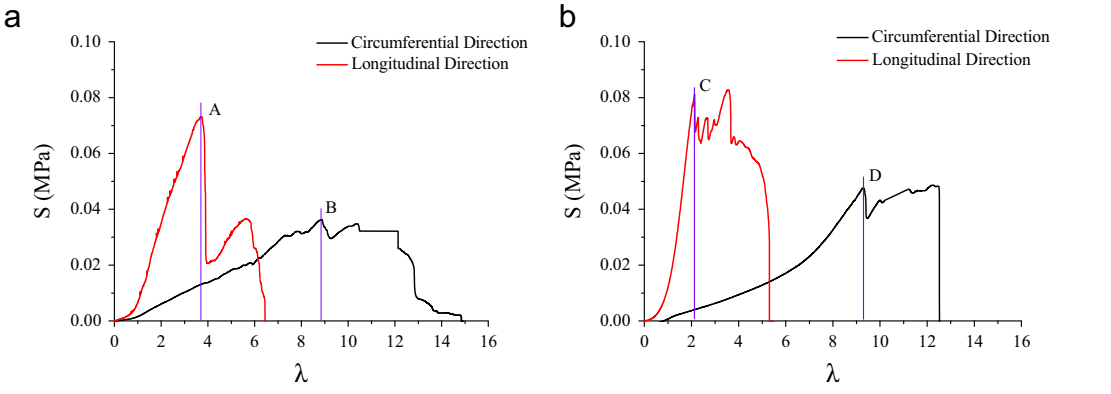

Failure points	A	B
S (MPa)	0.0728± 0.0034	0.0365± 0.0022
λ	3.385± 0.021	9.852± 0.031

Failure points	C	D
S (MPa)	0.0791± 0.0032	0.0411± 0.0025
λ	2.2811± 0.041	9.1811± 0.062

Fig. 6. Representative tensile failure stress-stretch ratio curves of stomach stripes at different orientations and locations, (a) Smaller curvature, (b) Greater curvature.

and soft tissue. The results of loading-unloading, stress relaxation, strain creep tests and fracture strength can been directly used to develop the mathematical and computational models in our future work to understand the biomechanical properties of stomach wall. In addition, in order to preferably explain the mechanical characteristics of the stomach tissue, we need to know the structure and function of the different locations and layers of gastric wall.

4.1. *Composite structure of gastric wall*

Fig. 7 shows the thickness of different layers from the greater and smaller curvature. The gastric wall in the greater curvature was thicker than that in the smaller curvature. The thickness of the serosa-muscle and mucosa-submucosa layer was almost same in the smaller curvature ($P < 0.05$), but the serosa-muscle layer

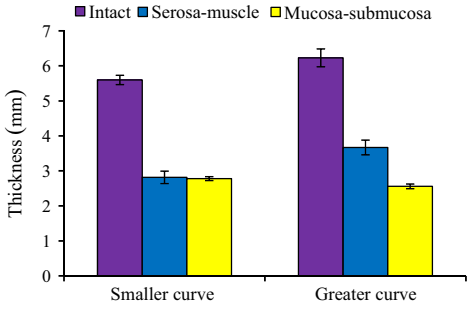

Fig. 7. Thickness of different layers from greater and smaller curvature.

was significantly thicker than the mucosa-submucosa layer in the greater curvature ($P > 0.05$). These results about gastric structure were very similar to that of Zhao et al.'s (2008). The differences were noticed only for mean thickness of gastric wall (5.8 mm in our work (Fig. 7) as compared to 6.5 mm in the work of Zhao). Hence, the tested porcine stomach had a composite structure, which induced the mechanical behaviors were different at different layers and locations.

4.2. Anisotropic mechanical behavior of gastric wall

The results in the present study showed that the mechanical properties of stomach were significantly different in the circumferential and longitudinal direction. In loading-unloading tests, the required stress for the serosa-muscle layer in the longitudinal direction was 15–20% more than that in the circumferential direction when the stretch ratio was 12%, but it could reach about 40% for the intact layer and 50% for the mucosa-submucosa layer. The results of stress relaxation and strain creep showed that the rate of variation was obviously faster in the circumferential direction than in the longitudinal direction, and the ultimate residual values were also different between the circumferential and the longitudinal direction when the duration reached 300 s. In the process of fracture tests, strips in the longitudinal direction firstly began to fracture and the required stress value was about twice as much as that in the circumferential direction. The above results indicated that the mechanical properties of stomach tissue were highly anisotropic. The study of Murtada et al. has shown that smooth muscles played an important mechanical role in the stomach and the orientation of smooth muscle myofilaments had a strong influence on the mechanical response of stomach (Murtada et al., 2010). Some studies indicated that smooth muscle tissues might produce a maximal force at an optimal length, which was larger than the slack length (Kamm et al., 1989). Van Loocke et al. observed the stiffening effect with compression rate especially in directions closer to the muscle fibers (Van Loocke et al., 2008). As the tested stripes in the longitudinal direction was parallel to the directions of gastric muscle fibres and mucosal fold, the tensile stress and stiffness in the longitudinal direction were always higher than that in the circumferential direction under the same stretch ratio.

4.3. Functions of gastric layered wall

The different mechanical behaviors in layered walls of the stomach were related to the various function of the stomach. The softer wall of the mucosa-submucosa could increase compliance and was thus suitable for accommodation. Similarly, gastric muscle grinded and mixed solid or liquid food within the stomach, and then moved it into the bowels at a controlled rate (Anupam et al., 2007). The various functions of gastric layer wall may result in their different responses to the stimuli. Furthermore, the nerve endings of the sensory afferent nerves in the gastric wall were located both in the submucosa and the muscle layers. According to the study, one of the most developed ganglionated plexuses of the gastrointestinal tract was the myenteric plexus located between the inner circular layer and outer longitudinal layer of the smooth muscle tunica. This suggests that the distributions of receptors from different layers in the wall may have different responses to the stimuli. According to the size of the area of their cell bodies, the neurons were divided as large, medium and small. In this way, 19.1% neurons were found to be large, 69.5% medium and 11.3%% small in fundus, 11.2% large, 80.6% medium and 8.7% small in body and 14.5% large, 74.3% medium and 11.1% small in pylorus (Saini and Gupta, 2007; Ozaki et al., 1999; Page et al., 2002; Zagoroonyuk et al., 2001). These studies suggest that the populations of receptors from different locations in the wall may have different responses to the stimuli.

Conflict of interest statement

None of the authors have any conflicts of interest with respect to the material contained in this manuscript.

Acknowledgment

This work was supported by National Natural Science Foundation of China (No. 51290291 and No. 51175440).

References

Anupam, P., James, G.B., Bertil, A., 2007. A stomach road or "Magenstrasse" for gastric emptying. J. Biomech. 40, 1202–1210.
Azpiroz, F., Malagelada, J.R., 1985. Physiologic variations in canine gastric tone measured by an electronic barostat. Am. J. Physiol. 248, G229–G237.
Bos, J., Doornebosch, E.W.L.J., Engbers, J.G., Nyhuis, O., Dodou, D., 2013. Methods for reducing peak pressure in laparoscopic grasping. Proc. Inst. Mech. Eng. H-J. Eng. Med. 227, 1292–1300.
De, S., Rosen, J., Dagan, A., Hannaford, B., Swanson, P., Sinanan, M., 2007. Assessment of tissue damage due to mechanical stresses. Int. J. Robotics Res. 26, 1159–1171.
Egorov, V.I., Schastlivtsev, I.V., Prut, E.V., Baranov, A.O., Turusov, R.A., 2002. Mechanical properties of the human gastrointestinal tract. J. Biomech. 35, 1417–1425.
Fung, Y.C., 1993. Biomechanics, Properties of living tissues. Springer-Verlag, Berlin.
Gregersen, H., Kassab, G., 2002. Biomechanics of the gastrointestinal tract. Neurogastroenterol. Motil. 8, 277–297.
Horowitz, M., Dent, J., Fraser, R., Sun, W., Hebbard, G., 1994. Role and integration of mechanisms controlling gastric-emptying. Dig. Dis. Sci. 39, S7–S13.
Kamm, K.E., Gerthoffer, W.T., Murphy, R.A., Bohr, D.F., 1989. Mechanical properties of carotid arteries from DOCA hypertensive swine. Hypertension 13, 102–109.
Liao, D.H., Zhao, J.B., Gregersen, H., 2005. Regional surface geometry of the rat stomach based on three-dimensional curvature analysis. Phys. Med. Biol. 50, 231–246.
Lyons, M., Winter, D.C., Simms, C.K., 2014. Mechanical characterisation of porcine rectus sheath under uniaxial and biaxial tension. J. Biomech. 47, 1876–1884.
Lyons, M., Winter, D.C., Simms, C.K., 2013. Extrusion properties of porcine intestines and surrogate materials for ventral hernia modelling. J. Mech. Behav. Biomed. Mater. 18, 57–66.
Marucci, D.D., Shakeshaft, A.J., Cartmill, J.A., Cox, M.R., Adams, S.G., Martin, C.J., 2000. Grasper trauma during laparoscopic cholecystectomy. Aust. N. Z. J. Surg. 70, 578–581.
Murtada, S.I., Kroon, M., Holzapfel, G.A., 2010. Modeling the dispersion effects of contractile fibers in smooth muscles. J. Mech. Phys. Solids 58, 2065–2082.
Ozaki, N., Sengupta, J.N., Gebhart, G.F., 1999. Mechanosensitive properties of gastric vagal afferent fibers in the rat. J. Neurophysiol. 82, 2210–2220.
Pal, A., Indireshkumar, K., Schwizer, W., Abrahamsson, B., Fried, M., Brasseur, J.G., 2004. Gastric flow and mixing studied using computer simulation. Proc. R. Soc. B-Biol. Sci. 271, 2587–2594.
Page, A.J., Martin, C.M., Blackshaw, L.A., 2002. Vagal mechanoreceptors and chemoreceptors in mouse stomach and esophagus. J. Neurophysiol. 87, 2095–2103.
Saini, N., Gupta, M., 2007. Morphometry of myenteric neurons in stomach. Nepal Med. Coll. J.: NMCJ 9, 96–99.
Van Loocke, M., Lyons, C.G., Simms, C.K., 2008. Viscoelastic properties of passive skeletal muscle in compression: stress-relaxation behaviour and constitutive modelling. J. Biomech. 41, 1555–1566.

Whitehead, W.E., Delvaux, M., Working, T., 1997. Standardization of barostat procedures for testing smooth tone and sensory thresholds in the gastrointestinal tract. Dig. Dis. Sci. 42, 223–241.
Zagoroonyuk, V.P., Chen, B.N., Brookes, X.J.H., 2001. Intraganglionic laminar endings are mechano-transduction sites of vagal tension receptors in the guinea-pig stomach. J. Physiol.-London 534, 255–268.
Zhao, J.B, Liao, D.H, Gregersen, H., 2005. Tension and stress in the rat and rabbit stomach are location-and direction-dependent. Neuroga stroenterol. Motil. 17, 388–398.
Zhao, J.B, Liao, D.H, Chen, P.M, Kunwald, P., Gregersen, H., 2008. Stomach stress and strain depend on location, direction and the layered structure. J. Biomech. 41, 3441–3447.